2009 American Control Conference
Hyatt Regency Riverfront, St. Louis, MO, USA
June 10-12, 2009

A further result on the optimal harmonic gait for locomotion of mechanical rectifier systems

J. Blair and T. Iwasaki

Abstract— **This paper first formally defines a general class of three dimensional rectifier systems which capture the essential aspects of animal locomotion, then formulates an optimal gait problem, and finally solves an approximation of the problem to obtain a globally optimal solution. The approximation assumes small-amplitude harmonic oscillations of mechanical joints about a nominal posture. The problem is formulated as a minimization of a quadratic cost function subject to an average velocity constraint, which is solved with an additional amplitude constraint in a Pareto-optimal fashion to ensure that the solution to the approximate problem is valid for the original. The solution method is fast and numerically stable, using generalized eigenvalues and eigenvectors of a pair of Hermitian matrices, and is able to easily handle underactuated or hyper-redundant systems. We provide case studies of a chain of links representing a radially symmetric jellyfish-like animal, or two limbs pushing a central body forward. It is demonstrated that our method enables determination of various gaits through optimization of such cost functions as input power, rate of shape change, and torque derivative.**

I. Introduction

Currently, there are many situations in which existing vehicular machines are poorly suited, due to their limited ability to adapt to varying terrain and maneuver in confined spaces. Many animals possess a high degree of adaptability and maneuverability, and the mechanisms they employ to locomote may provide a framework for designing highly functional mobile robots. We view animal locomotion as mechanical rectification, a process that converts a rhythmic gait into a biased velocity through interaction with the environment. A fundamental problem is the determination of a gait for a given mechanical rectifier which achieves a desired velocity while minimizing a given criterion. It is also essential to ensure achievability of the gait with the given set of actuators in the solution process.

There are many approaches for determining optimal gaits for robotic locomotors in literature. Some parameterize a gait observed in biology and use gridding with simulation to minimize a given criterion. This approach has been used to determine gaits for human walking [1], snake crawling [2], and anguilliform swimming [3]. Gridding and simulation are slow, however, and a parameterized set may exclude "unnatural" gaits having better performance than those observed in biology. Others find optimal gaits based on standard formulations of optimal control problems and various combinations of existing optimization methods. One such method is to reduce the problem to a parametric optimization by expanding the signals over a finite set of basis functions. This approach has been used to determine gaits for eel swimming [4] and biped walking [5]. Some use the calculus of variations to reduce the problem to a two-point boundary-value problem. This approach has been used for nonholonomic locomotion systems [6], a seven-link biped robot [7], and shape actuated locomotion systems [8]. The main limitation of the current methods is their locally optimal nature, which may generate a solution far from the global optimum depending on choice of initial conditions.

In this paper, we provide a fast and numerically stable method to determine a globally optimal solution to an approximate locomotion problem, instead of providing a locally optimal solution to the general problem. The method also ensures achievability and can be easily applied to underactuated or hyper-redundant systems. We will first formally define a class of multibody rectifier systems that capture the essential aspects of animal locomotion, then formulate a general optimal gait problem. The problem is approximated assuming small-amplitude harmonic oscillations about a nominal posture, and then finally solved using generalized eigenvalues and eigenvectors of a pair of Hermitian matrices.

The present paper extends our previous result [9] in several aspects. While we considered planar motion of rigid body rectifiers earlier, the class of rectifier systems is now described in three dimensional space and includes those with flexible joints. The stiffness of the body broadens the set of possible nominal postures by providing the force required to balance out the average environmental force during locomotion. The quadratic cost function for the optimal gait problem is also generalized to include dynamic (as opposed to constant) weighting matrices, encompassing an extended list of performance indices. We show how an efficiency measure can be minimized under an additional constraint on the amplitude of oscillation to ensure that the solution to the approximate system is valid. Case studies are given for a chain of flexible links representing a radially symmetric jellyfish-like animal. It is demonstrated that our method enables determination of various gaits through optimization of such cost functions as input power, rate of shape change, and torque derivative.

II. Rectifier systems

The following sections describe the general equations of motion for rectifier systems and their approximations.

J. Blair and T. Iwasaki are with Department of Mechanical and Aerospace Engineering, University of Virginia, 122 Engineer's Way, Charlottesville, VA 22904 USA, {jtb8s,iwasaki}@virginia.edu

978-1-4244-4524-0/09/$25.00 ©2009 AACC

A. Rectifier Equations of Motion

Consider a general multi-body mechanical system, actuated at selected flexible joints, that interacts with a surrounding environment through the motion of its bodies. We call such systems mechanical rectifiers when periodic motion of the body can result in locomotion (bulk displacement of the center of mass of the system). We restrict our attention to systems that *continually* interact with the environment. This excludes systems such as walking robots but still includes a wide range of other animal locomotions, such as swimming, crawling (such as in snakes), and flying. The swimming limbed animal depicted in Fig. 1 is one such example.

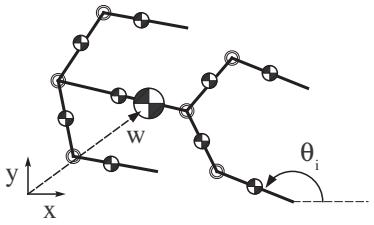

Fig. 1. Multilink swimming system

The general equations of motion are given by

$$\begin{aligned} &J_\theta\ddot{\theta} + G_{\theta,\dot{\theta}}\dot{\theta} + d_{\dot{\theta}} + k_\theta + R_\theta^\intercal\gamma(R_\theta\dot{\theta} + N_\theta v) = Bu, \\ &m\dot{v} + N_\theta^\intercal\gamma(R_\theta\dot{\theta} + N_\theta v) = 0, \end{aligned} \tag{1}$$

where $\theta(t) \in \mathbb{R}^n$ are the generalized coordinates for the body shape and orientation, $v(t) \in \mathbb{R}^k$ is the velocity of the center of mass, $u(t) \in \mathbb{R}^\ell$ are the torque inputs at selected joints, and k =1, 2, or 3 is the number of spacial dimensions. The subscripts indicate dependence of the matrices and vectors on the variables. The terms $J_\theta\ddot{\theta} + G_{\theta,\dot{\theta}}\dot{\theta}$ and $m\dot{v}$ are the inertial torques and forces, and $d_{\dot{\theta}} + k_\theta$ is the joint torques due to damping and stiffness. R_θ and N_θ are position dependent matrices that transform the global velocity components into local body coordinates. The function $\gamma : \mathbb{R}^p \to \mathbb{R}^p$ is a possibly nonlinear mapping that generates the forces and torques (in local body coordinates) resulting from the relative motion of the system with the environment. Typically, γ satisfies the sector condition $y_i x_i \geq 0$ for each entry of the input/output pair $y = \gamma(x)$. The quantity $R_\theta^\intercal\gamma(R_\theta\dot{\theta} + N_\theta v)$, therefore, is the vector of forces and torques in the global frame as a function of the link velocities $(R_\theta\dot{\theta} + N_\theta v)$ in the body coordinates relative to the environment.

B. Nominal Posture and Bilinear Approximation

We assume that a rectifier system possesses a *nominal posture*, $\theta(t) \equiv \eta \in \mathbb{R}^n$, which is a set of shape variables that, given a specific velocity v_o of the center of mass, simultaneously maintain the direction of motion (but not magnitude) and body shape in the absence of any actuating input u. In other words, actuation is not required to maintain body shape and orientation if the system is moving at velocity v_o. Actuation is needed to counter bulk environmental drag and maintain the velocity at v_o, however. More specifically, we expect that periodic body motion about η will produce the necessary thrust for the system to remain moving at the average velocity v_o in the steady state. A nominal posture must therefore satisfy

$$R_\eta^\intercal\gamma(N_\eta v_o) + k_\eta = 0, \quad N_\eta^\intercal\gamma(N_\eta v_o) \in \mathbb{V}, \tag{2}$$

where $\mathbb{V}$ is the straight line in $\mathbb{R}^k$ that is parallel to v_o and passes through the origin, indicating the direction of locomotion. Throughout the paper, we choose the global coordinate frame so that its first axis is aligned with $\mathbb{V}$, that is, $v_o = v_x e_1$ for some $v_x \in \mathbb{R}$ where $e_i \in \mathbb{R}^k$ is the vector whose i^{th} entry is one and the others are zero.

To gain insight into the problem, we attempt to analyze the behavior of the rectifier system through the simplest approximate model that captures the essential dynamics of rectification. Thus, we restrict our attention to those systems for which it is reasonable to approximate the interactive force by a linear function (through such methods as standard linearization and describing function), i.e., $\gamma(x) \cong \Gamma x$ for a constant matrix Γ. Furthermore, we consider small amplitude oscillations about the nominal posture $\vartheta := \theta - \eta$ at an average steady state velocity. We use the approximations

$$\begin{aligned} &N_\theta^\intercal\Gamma N_\theta = C_\vartheta + \mathsf{O}(\vartheta^3), \quad &&J_\theta = J + \mathsf{O}(\vartheta), \\ &R_\theta^\intercal\Gamma R_\theta = D_1 + \mathsf{O}(\vartheta), \quad &&k_\theta = k_\eta + K\vartheta + \mathsf{O}(\vartheta^2), \\ &R_\theta^\intercal\Gamma N_\theta = E_\vartheta + \mathsf{O}(\vartheta^2), \quad &&d_{\dot{\theta}} = D_2\dot{\vartheta} + \mathsf{O}(\dot{\vartheta}^2) \end{aligned}$$

where J, D_1, D_2, and K are constants, E_ϑ is affine in ϑ, and C_ϑ is quadratic in ϑ. Assuming that $v(t) \approx v_o$, we obtain

$$\begin{aligned} &J\ddot{\vartheta} + D\dot{\vartheta} + K\vartheta + L_\vartheta v = Bu, \\ &m\dot{v} + E_\vartheta^\intercal\dot{\vartheta} + C_\vartheta v = 0, \end{aligned} \tag{3}$$

where $D := D_1 + D_2$ and $L_\vartheta := E_\vartheta - E_0$. We linearized the first equation in (1) in terms of ϑ and kept terms up to the second order in ϑ in the second equation as the essential mechanism for rectification would have otherwise been lost.

III. Optimal Locomotion

In this section, we formulate an optimal locomotion problem for the mechanical rectifier (3) and provide a solution.

A. Problem formulation

We consider the optimal locomotion problem of minimizing a quadratic cost function over the set of T-periodic signals $\mathbb{S}_T$, subject to the constraint that the average speed of locomotion is v_o:

$$\begin{aligned} \min_{\substack{T \in \mathbb{R}_+ \\ v,\vartheta,u \in \mathbb{S}_T}} \quad & \frac{1}{T}\int_0^T \begin{bmatrix} \vartheta \\ u \end{bmatrix}^\intercal \Pi \begin{bmatrix} \vartheta \\ u \end{bmatrix} dt \\ \text{s.t.} \quad & \begin{cases} \dfrac{1}{T}\displaystyle\int_0^T v dt = v_o, \\ J\ddot{\vartheta} + D\dot{\vartheta} + K\vartheta + L_\vartheta v = Bu, \\ m\dot{v} + E_\vartheta^\intercal\dot{\vartheta} + C_\vartheta v = 0. \end{cases} \end{aligned} \tag{4}$$

where Π is a linear time invariant operator represented by its transfer function $\hat{\Pi}(s)$. Without loss of generality, we assume $v_o = v_x e_1$ for some $v_x \in \mathbb{R}$.

The objective function is quadratic in ϑ and u, and through the choice of Π, derivatives of ϑ and u may also be captured,

TABLE I

OBJECTIVE FUNCTIONS SPECIFIED BY Π

Quantity	Objective Integral	$\hat{\Pi}(j\omega)$
Perturbation from η	$\frac{1}{T}\int_0^T \|\vartheta\|^2 dt$	$\begin{bmatrix} I & 0 \\ 0 & 0 \end{bmatrix}$
Joint Deflection	$\frac{1}{T}\int_0^T \|\phi\|^2 dt$	$\begin{bmatrix} W^\mathsf{T}W & 0 \\ 0 & 0 \end{bmatrix}$
Bending Rate	$\frac{1}{T}\int_0^T \|\dot{\phi}\|^2 dt$	$\begin{bmatrix} \omega^2 W^\mathsf{T}W & 0 \\ 0 & 0 \end{bmatrix}$
Input Torque	$\frac{1}{T}\int_0^T \|u\|^2 dt$	$\begin{bmatrix} 0 & 0 \\ 0 & I \end{bmatrix}$
Input Torque Rate	$\frac{1}{T}\int_0^T \|\dot{u}\|^2 dt$	$\begin{bmatrix} 0 & 0 \\ 0 & \omega^2 I \end{bmatrix}$
Input Power	$\frac{1}{T}\int_0^T \dot{\theta}^\mathsf{T} B u dt$	$\frac{1}{2}\begin{bmatrix} 0 & -j\omega B \\ j\omega B^\mathsf{T} & 0 \end{bmatrix}$

representing many physical quantities such as input power. Table I provides a short list of such quantities and their associated $\hat{\Pi}(j\omega)$ values, where $\phi := W\theta$ is the vector of joint angles specified by W. The average value over one period is taken for input power, and mean-square values for the other quantities.

For tractability, we shall reformulate the problem in (4) by restricting the underlying class of periodic signals. In particular, the search for the optimal gait is confined to the class of T-periodic, unbiased, harmonic signals $\mathbb{H}_T$. Assuming that $v \approx v_o$ and averaging the third constraint in (4), we obtain

$$\int_0^T \Big((a_i + \vartheta^\mathsf{T} C_i \vartheta) v_x + \dot{\vartheta}^\mathsf{T} \Lambda_i \vartheta dt \Big) = 0, \tag{5}$$

for $i = 1, ..., k$, where a_i, C_i, and Λ_i are specified by

$$L_\vartheta e_i = \Lambda_i \vartheta, \;\; e_i^\mathsf{T} C_\vartheta e_1 = a_i + b_i^\mathsf{T}\vartheta + \vartheta^\mathsf{T} C_i \vartheta.$$

Let us now define the following problem:

$$\begin{array}{l} \min\limits_{\substack{T \in \mathbb{R}_+ \\ \vartheta,\, u \in \mathbb{H}_T}} \; \dfrac{1}{T}\displaystyle\int_0^T \begin{bmatrix} \vartheta \\ u \end{bmatrix}^\mathsf{T} \Pi \begin{bmatrix} \vartheta \\ u \end{bmatrix} dt \\ \quad \text{s.t.} \; \left\{ \begin{array}{l} \displaystyle\int_0^T \Big((a_1 + \vartheta^\mathsf{T} C_1 \vartheta) v_x + \dot{\vartheta}^\mathsf{T} \Lambda_1 \vartheta dt \Big) = 0, \\ J\ddot{\vartheta} + D\dot{\vartheta} + K\vartheta + v_x \Lambda_1 \vartheta = Bu. \end{array} \right. \end{array} \tag{6}$$

We expect that a solution to this problem will automatically satisfy the remaining omitted acceleration constraints, i.e., (5) for $i = 2, \ldots, k$, on the grounds that acceleration in a direction normal to $\mathbb{V}$ would require a larger objective value and would hence be eliminated. This is also what we have observed in all of our numerical studies.

B. Harmonic solution

This section presents an exact solution to the problem in (6). The following lemma reduces the problem to a constrained quadratic optimization.

Lemma 1: *Consider the problem in (6). Define*

$$\begin{array}{l} X_\omega := \begin{bmatrix} P_\omega \\ I \end{bmatrix}^* \hat{\Pi}(j\omega) \begin{bmatrix} P_\omega \\ I \end{bmatrix}, \\ Y_\omega := P_\omega^* \left(j(\omega/v_o)(\Lambda_1 - \Lambda_1^\mathsf{T}) - 2C_1 \right) P_\omega / (4a_1), \\ P_\omega := (v_x \Lambda_1 + K + j\omega D - \omega^2 J)^{-1} B. \end{array} \tag{7}$$

Then the problem is equivalent to

$$\min_{\omega \in \mathbb{R},\; \hat{u} \in \mathbb{C}^\ell} \; \{ \; \hat{u}^* X_\omega \hat{u} : \; \hat{u}^* Y_\omega \hat{u} = 1 \; \}. \tag{8}$$

Proof: The problem in (6) can be rewritten in terms of phasors as follows:

$$\begin{array}{l} \min\limits_{\substack{\omega \,\in\, \mathbb{R} \\ \hat{\vartheta} \,\in\, \mathbb{C}^n,\; \hat{u} \,\in\, \mathbb{C}^\ell}} \begin{bmatrix} \hat{\vartheta} \\ \hat{u} \end{bmatrix}^* \hat{\Pi}(j\omega) \begin{bmatrix} \hat{\vartheta} \\ \hat{u} \end{bmatrix} \\ \quad \text{s.t.} \; \left\{ \begin{array}{l} (2a_1 + \hat{\vartheta}^* C_1 \hat{\vartheta}) v_x + \Re[(j\omega\hat{\vartheta})^* \Lambda_1 \hat{\vartheta}] = 0, \\ (-\omega^2 J + j\omega D + K + v_x \Lambda_1)\hat{\vartheta} = B\hat{u}. \end{array} \right. \end{array}$$

The second constraint can be solved for $\hat{\vartheta} = P_\omega \hat{u}$. Using this expression for ϑ in the objective function, the second constraint can be eliminated to yield (8). ∎

In (8), the vector $\hat{u}$ is the phasor of the input signal $u(t)$. Hence, once (8) is solved for a minimizer $(\omega, \hat{u})$, the optimal sinusoidal input for (6) can be found as $u(t) = \Re[\hat{u} e^{j\omega t}]$. To solve the problem in (8), one may optimize over $\hat{u}$ for a fixed ω, and repeat this process for various values of ω, numerically sweeping the frequency axis. In this case, each problem for a given ω is a static quadratic optimization, which is nonconvex in general because X_ω and Y_ω are possibly indefinite. Nonconvex optimizations are often hard to solve, but for this particular problem, we have a complete solution as shown in [9].

Lemma 2: *Let Hermitian matrices X and Y be given and consider*

$$\min_{q \in \mathbb{C}^\ell} \; \{ \; q^* X q : \; q^* Y q = 1 \; \}. \tag{9}$$

The constraint is feasible if and only if the largest eigenvalue of Y is positive. In this case, the objective function is bounded below on the feasible set if and only if the following (convex) set is nonempty:

$$\mathbb{L} := \{ \; \lambda \in \mathbb{R} : \; X \geq \lambda Y \; \}.$$

The largest element λ_o of $\mathbb{L}$ is well defined and is a generalized eigenvalue of (X, Y). The minimum value of (9) is equal to λ_o. An optimizer q_o is given by an eigenvector of the pair (X, Y) associated with the generalized eigenvalue λ_o, normalized so that $q_o^* Y q_o = 1$.

Based on Lemma 2, a solution to (9) can be found by computing the generalized eigenvalues of (X, Y). If the constraint is feasible and objective function is bounded, then one (or more) of the generalized eigenvalues must be real and satisfy $X \geq \lambda Y$. The largest of such generalized eigenvalues is λ_o. If λ_o is not repeated, then it has one-dimensional eigenspace. In this case, every eigenvector q_o satisfies $q_o^* Y q_o > 0$ and hence can be normalized so that $q_o^* Y q_o = 1$. This q_o is an optimizer of (9). If λ_o is repeated, then the dimension of the eigenspace is more than one and $q_o^* Y q_o$ can be nonpositive for some eigenvector. However, Lemma 2 guarantees that at least one of them gives positive $q_o^* Y q_o$ and hence is a solution after the normalization.

Combining Lemmas 1 and 2, we have the following result that solves the problem in (6).

Theorem 1: *Consider the rectifier system given in (3) and the optimal locomotion problem in (6). Define X_ω, Y_ω, and P_ω by (7). Let γ be the optimal value of the objective function. Then we have*

$$\gamma = \min_{\omega\in\mathbb{R}} \max_{\lambda\in\mathbb{R}} \ \{\ \lambda :\ X_\omega \geq \lambda Y_\omega\ \}. \tag{10}$$

Let ω_o and λ_o be the optimizers. Then, the optimal period is $T = 2\pi/\omega_o$, and the optimal input and body angles are given by

$$u(t) = \Re[q_o e^{j\omega_o t}],\ \ \vartheta(t) = \Re[P_{\omega_o} q_o e^{j\omega_o t}],$$

where $q_o \in \mathbb{C}^\ell$ is an eigenvector of the pair $(X_{\omega_o}, Y_{\omega_o})$ associated with the generalized eigenvalue λ_o, normalized to satisfy $q_o^* Y_{\omega_o} q_o = 1$.

The problem in (10) can be solved by generalized eigenvalue computation plus a line search. For a fixed ω, the optimal solution is obtained from the maximization of λ, which is given in terms of a generalized eigenvalue of (X, Y).

C. Some ideas on implementation

Most animals have a body symmetric about an axis (or a plane), and the direction of locomotion is often chosen to be aligned with the axis of symmetry. A robotic locomotor may be designed to have this property. In this case, feasible gaits may be restricted to be symmetric about the $\mathbb{V}$ line, at the expense of potential increase in the cost function value. A benefit is that the symmetry can be exploited to make the gait optimization simpler. A symmetric gait would automatically lead to locomotion along the $\mathbb{V}$ line due to the balance of forces. The equations of motion (3) can then be given in terms of a reduced number of independent variables. For an example, the locomotor in Fig. 1 could be reduced to the system shown in Fig. 2. The reduction in the size of the optimization problem (the dimension of X_ω) would generally lead to more efficient and reliable computation.

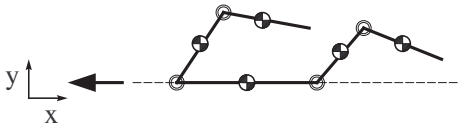

Fig. 2. Symmetric reduction of multilink system

For the quadratic cost function with an arbitrary weighting Π_o, the solution to (6) may generate a gait with a large amplitude oscillation of ϑ, violating the small amplitude assumption imposed to derive the bilinear equations of motion in (3). Such gait may not be appropriate for the original equations of motion (1) and may not make physical sense. To remedy this situation, one can penalize the amplitude of ϑ by setting

$$\Pi = (1-\beta)\Pi_{\rm amp} + \beta\Pi_o,$$

where $\Pi_{\rm amp}$ corresponds to the first entry in Table I, and β is a weighting parameter satisfying $0 \leq \beta \leq 1$. When $\Pi_{\rm amp}$ and Π_o define competing objectives, the amplitude of optimal ϑ would be a nondecreasing function of β. The largest value of β is thus found so as to satisfy a hard constraint on the amplitude of ϑ. This type of Pareto-optimal approach has been used for multiobjective H_2 control with a proof of convergence [10].

IV. Case studies

In this section, we illustrate the optimal locomotions for a specific example. We consider planar motion of a single chain of links in water, modeled by (1) and (3) with definitions given in the appendix. The precise values of the parameters are not important, however we use measured data of a medium size leech to keep the model realistic. The leech has mass $m = 1.1$ g and length $\ell = 107.3$ mm, and swims by undulating its slender body like snakes at speed around 0.15 m/s. The leech body is modeled by a chain of n identical links where $n = 18$, with all $n-1$ joints actuated.

For the chain of links, there can be multiple nominal postures around which body oscillations occur. One choice is a straight chain $\eta = 0$ for undulatory locomotion as in leeches. This configuration qualifies as a nominal posture for any locomotion speed with or without joint stiffness, and has been considered in our previous study [9]. Another choice would be a "U" shaped bend, which can be thought of as two flagella pushing a central body forward, or a radially symmetric jellyfish-like animal. This is the nominal posture we consider here. Assuming an average velocity of $v_x = -0.1$ m/s (negative sign indicates swimming to the left), the joint stiffness function k_θ has been determined so that $k_\theta = B\mathsf{K}B^{\mathsf{T}}\theta$ for some diagonal K with nominal posture η given by η_i linearly decreasing from $\eta_1 = \pi - 0.068$ to $\eta_n = 0.068$ rad.

We have solved the optimal gait problem in (6) for $v_x = -0.1$ m/s with some objective functions from Table I. For each case, the problem is reformulated as in (8), with an additional hard constraint on the amplitude $\|\hat{\vartheta}\|^2 \leq 10$. The problem is then solved using the Pareto-optimal approach described in Section III-C.

We examine three cases: minimum power, bending rate, and rate of input torque, as specified in Table I. Power is often important in robot design, and one would expect it to probably be minimized in biological animals. If there is a very high cost associated with the rate of joint deflection (high joint damping for example), the rate of bending would be minimized. Finally, biology inspires us to examine the rate of input torque, based on the idea that this correlates to the *intent* to move, which might capture expensive chemical processes in muscle activation and deactivation. The results of the three optimizations are summarized in terms of $\varphi := B^{\mathsf{T}}\vartheta$, which are the joint angle deflections from the nominal posture. Numerical simulations are then used to examine the effects of approximations associated with the equations of motion and the optimal gait problem. Unless otherwise noted, the second equation in (3) is simulated by enforcing the calculated optimal gait $\theta(t)$ as the input.

Figure 3 shows the phase and amplitude of φ for the three optimal gaits whose frequencies are summarized in Table II. We see that the phase is maximum at or around the center and decreases toward both ends. This means that all three gaits possess some degree of traveling waves down each arm. However, the minimum bending rate motion has a much smaller phase variation than the power or torque rate case, indicating that it has a much lower number of waves expressed along the body. It should be noted that the rate of input torque generated an asymmetric result. After checking this result against the optimal gait under the symmetry constraint, we found that the asymmetric gait did indeed have a strictly smaller minimum objective value. Among the three cases, the average amplitude over the body tends to be smaller if the phase variation is smaller. This is because small, relatively in-phase, joint angle amplitudes add up to produce a large overall motion which maintains the desired velocity. Interestingly, the torque rate case does not bend at all at the center joint (only rotates), retaining its initial nominal bend at all times.

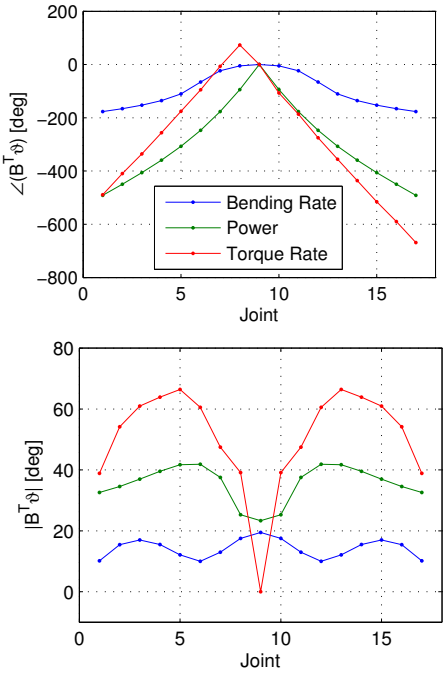

Fig. 3. Optimal gaits

Figure 4 shows five snapshots of simulated optimal locomotion for each case, taken 1.2 periods apart. The optimal motion calculated for minimum power and bending rate are symmetric about the direction of locomotion (horizontal axis). The asymmetry is clearly visible for the torque rate case. The horizontal axis scales are different in each figure due to the differing optimal frequencies calculated for each motion; for example the bending rate motion moves much further in five periods than the torque rate motion, although the locomotion speeds are about the same.

Figure 5 shows the simulated velocity, where the time responses are colored in the same way as Fig. 3 for each case.

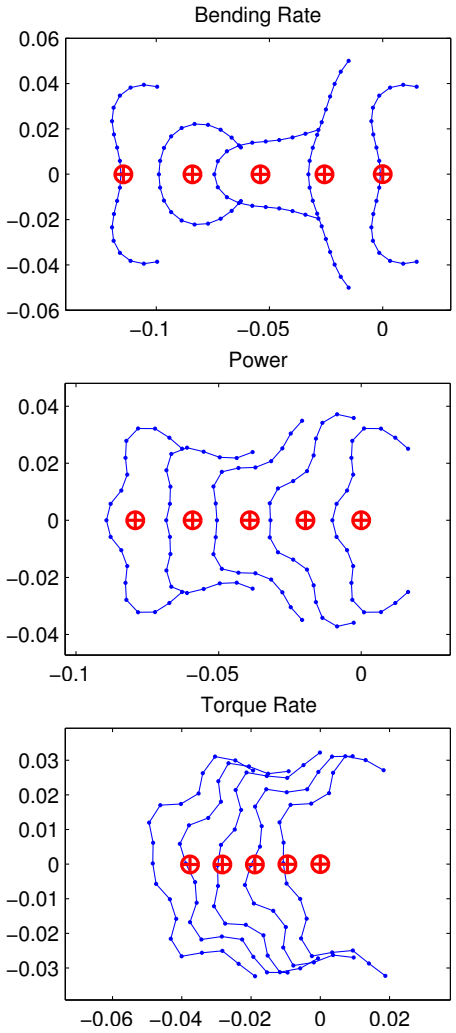

Fig. 4. Snap shots of locomotion

We see that v_y is exactly zero for the symmetric motions, and oscillating closely about zero for the asymmetric case. The oscillation of v_x is small in the power and torque rate cases, but is much larger in the bending rate case due to the large stroking motion of the arms. The non-sinusoidal shape in the bending rate case results from higher frequency components which can be explained by thinking of a flipping fish tail: for one period of motion the tail produces two thrusts. The varying v_x magnitude results from the alternating high and low drag associated with the arms being extended out or folded back during the stroke. In general, the higher the wave number and frequency a motion possesses, the smaller the perturbation about the average velocity.

Finally, average velocities are summarized in Table II. The nonlinear and bilinear velocities are simulated from the second equation in (1) and (3), respectively. For the bilinear case, the simulated average velocities are close to $v_x = -0.1$ m/s at which the optimal gaits are calculated, despite the fact that oscillations of v_x around this value are ignored during the optimization. On the other hand, the higher order nonlinearity tends to reduce the actual swim speed.

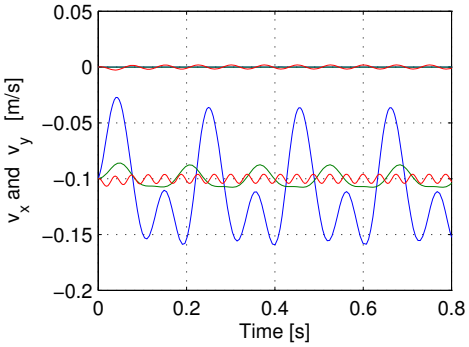

Fig. 5. Simulated CG velocity

TABLE II

OPTIMAL FREQUENCIES [rad/s] AND SIMULATED VELOCITIES [mm/s]

Quantity	Optimal ω	Nonlinear v_x	Bilinear v_x
Power	39.7	-69.8	-100.7
Bending Rate	30.5	-82.8	-107.9
Torque Rate	83.9	-67.4	-100.3

V. CONCLUSION

This paper has extended a previous paper [9] to include a more general class of three dimensional rectifier systems and nominal postures. First, an optimal locomotion problem was formulated as minimization of a quadratic cost function subject to an average velocity constraint. A globally optimal solution was then obtained for an approximation of the problem where we assumed small perturbations about a nominal posture and a restriction to harmonic variables. The solution satisfied an additional amplitude constraint through the choice of objective function in a Pareto-optimal fashion to ensure that the solution to the approximate system was valid. The solution was reduced to calculation of generalized eigenvalues and eigenvectors of a pair of Hermitian matrices as frequency was varied, resulting in a very fast and numerically stable method capable of handling underactuated and hyper-redundant systems while ensuring achievability.

The case studies have shown that the quadratic optimization can produce gaits that closely resemble those seen in biology. Most optimal gaits were found to be symmetric, agreeing with our intuition based on biological observations of swimming animals. The gait which minimized the torque derivative was found to be asymmetric, however, indicating that some systems may benefit from unconventional gaits that are not commonly observed in biology and counter to intuition. Finally, these studies demonstrate that the proposed framework for computing optimal gaits can be very useful for increasing our understanding of animal locomotion mechanisms from a biological point of view.

Acknowledgments: The authors thank Professor W.O. Friesen and Ms. J. Chen at the University of Virginia for providing the measured data for a leech. This work is supported by the Office of Naval Research, under MURI Grant N00014-08-1-0642, and by the National Science Foundation under No.0654070.

APPENDIX

Locomotor model parameter values:

$$n = 18, \quad m = 0.0011 \ \mathrm{kg}, \quad \ell = 0.1073 \ \mathrm{m},$$
$$c_{n_i} = 0.8\ell_i \ \mathrm{N \cdot s/m}, \quad c_{t_i} = 0.1\ell_i \ \mathrm{N \cdot s/m},$$
$$m_i = m/n, \quad \ell_i = \ell/(2n), \quad J_i := m_i\ell_i^2/3, \quad D_J = 0.$$

Definitions of parameters in nonlinear rectifier (1):

$$J_\theta := J + \mathrm{S}_\theta H \mathrm{S}_\theta + \mathrm{C}_\theta H \mathrm{C}_\theta, \quad G_\theta := \mathrm{S}_\theta H \mathrm{C}_\theta - \mathrm{C}_\theta H \mathrm{S}_\theta,$$
$$R_\theta := \begin{bmatrix} \Omega_\theta L_\theta \\ I \end{bmatrix}, \quad N_\theta := \begin{bmatrix} \Omega_\theta E \\ 0 \end{bmatrix},$$
$$L_\theta := \begin{bmatrix} F\mathrm{S}_\theta \\ -F\mathrm{C}_\theta \end{bmatrix}, \quad \Omega_\theta := \begin{bmatrix} \mathrm{C}_\theta & \mathrm{S}_\theta \\ -\mathrm{S}_\theta & \mathrm{C}_\theta \end{bmatrix}, \quad E := \begin{bmatrix} e & 0 \\ 0 & e \end{bmatrix},$$
$$\mathrm{S}_\theta := \mathrm{diag}(\sin\theta_1, \ldots, \sin\theta_n), \quad e := \begin{bmatrix} 1 & \ldots & 1 \end{bmatrix}^\mathsf{T} \in \mathbb{R}^n,$$
$$\mathrm{C}_\theta := \mathrm{diag}(\cos\theta_1, \ldots, \cos\theta_n), \quad J := \mathrm{diag}(J_1, \ldots, J_n),$$
$$H := LA(B^\mathsf{T}M^{-1}B)^{-1}A^\mathsf{T}L, \quad M := \mathrm{diag}(m_1, \ldots, m_n),$$
$$F := M^{-1}B(B^\mathsf{T}M^{-1}B)^{-1}A^\mathsf{T}L, \quad L := \mathrm{diag}(\ell_1, \ldots, \ell_n),$$
$$C_t := \mathrm{diag}(c_{t_1}, \ldots, c_{t_n}), \quad C_n := \mathrm{diag}(c_{n_1}, \ldots, c_{n_n}),$$
$$\gamma(x) := \Gamma x, \quad \Gamma := \mathrm{diag}(C_t, C_n, C_n L^2/3),$$
$$A := \begin{bmatrix} 1 & 1 & & \\ & \ddots & \ddots & \\ & & 1 & 1 \end{bmatrix}^\mathsf{T}, \quad B := \begin{bmatrix} 1 & -1 & & \\ & \ddots & \ddots & \\ & & 1 & -1 \end{bmatrix}^\mathsf{T},$$
$$d_{\dot\theta} = BD_JB^\mathsf{T}\dot\theta, \quad D_J := \mathrm{diag}(d_1, \ldots, d_n),$$
$$k_\theta = BK_JB^\mathsf{T}\theta, \quad K_J := \mathrm{diag}(k_1, \ldots, k_n).$$

Definitions of parameters in bilinear rectifier (3):

$$J := J_\eta, \quad D := BD_JB^\mathsf{T} + R_\eta^\mathsf{T}\Gamma R_\eta, \quad L_\vartheta := \begin{bmatrix} \Lambda_1\vartheta & \Lambda_2\vartheta \end{bmatrix},$$
$$C_\vartheta := N_\eta^\mathsf{T}\Gamma N_\eta + B_\vartheta + \Theta^\mathsf{T}C\Theta, \quad \Theta := \mathrm{diag}(\vartheta, \vartheta),$$
$$B_\vartheta := N_\eta^\mathsf{T}\Gamma N_1\Theta + (N_\eta^\mathsf{T}\Gamma N_1\Theta)^\mathsf{T},$$
$$C := N_1^\mathsf{T}\Gamma N_1 + R_C + R_C^\mathsf{T}, \quad \Omega_2 := -\Omega_\eta/2,$$
$$R_C := \begin{bmatrix} \mathrm{diag}(\bar r_1) & \mathrm{diag}(\bar r_2) \\ \mathrm{diag}(\bar r_3) & \mathrm{diag}(\bar r_4) \end{bmatrix}, \quad \begin{bmatrix} \bar r_1 & \bar r_2 \\ \bar r_3 & \bar r_4 \end{bmatrix} := N_\eta^\mathsf{T}\Gamma N_2,$$
$$\begin{bmatrix} \Lambda_1 & \Lambda_2 \end{bmatrix} := \begin{bmatrix} \mathrm{diag}(\bar v_1) & \mathrm{diag}(\bar v_2) \end{bmatrix} + R_\eta^\mathsf{T}\Gamma N_1 + R_{1\Omega}^\mathsf{T}\Gamma N_o,$$
$$\begin{bmatrix} \bar v_1 & \bar v_2 \end{bmatrix} := R_{1L}^\mathsf{T}\Gamma N_\eta,$$
$$R_{1L} := \begin{bmatrix} \Omega_\eta L_1 \\ 0 \end{bmatrix}, \quad R_{1\Omega} := \begin{bmatrix} \Omega_1 L_\eta \\ 0 \end{bmatrix},$$
$$\Omega_1 := \begin{bmatrix} -\mathrm{S}_\eta & \mathrm{C}_\eta \\ -\mathrm{C}_\eta & -\mathrm{S}_\eta \end{bmatrix}, \quad L_1 := \begin{bmatrix} F\mathrm{C}_\eta \\ F\mathrm{S}_\eta \end{bmatrix},$$
$$N_o := \begin{bmatrix} \Omega_\eta \\ 0 \end{bmatrix}, \quad N_1 := \begin{bmatrix} \Omega_1 \\ 0 \end{bmatrix}, \quad N_2 := \begin{bmatrix} \Omega_2 \\ 0 \end{bmatrix}.$$

REFERENCES

[1] C. Chevallereau and Y. Aoustin. Optimal reference trajectories for walking and running of a biped robot. *Robotica*, 19:557–569, 2001.

[2] M. Saito, M. Fukaya, and T. Iwasaki. Serpentine locomotion with robotic snake. *IEEE Control Systems Magazine*, 22(1):64–81, 2002.

[3] K.A. McIsaac and J.P. Ostrowski. Motion planning for anguilliform locomotion. *IEEE Trans. Robotics and Automation*, 19(4):637–652, 2003.

[4] J. Cortes, S. Martinez, J.P. Ostrowski, and K.A. McIsaac. Optimal gaits for dynamic robotic locomotion. *The International journal of robotics research*, 20(9):707–728, 2001.

[5] T. Saidouni and G. Bessonnet. Generating globally optimised sagittal gait cycles of a biped robot. *Robotica*, 21(2), 2003.

[6] J.P. Ostrowski, J.P. Desai, and V. Kumar. Optimal gait selection for nonholonomic locomotion systems. *The International journal of robotics research*, 19:225–237, 2000.

[7] G. Bessonnet, S. Chesse, and P. Sardain. Optimal gait synthesis of a seven-link planar biped. *The International journal of robotics research*, 23(10-11):1059–1073, 2004.

[8] G. Hicks and K. Ito. A method for determination of optimal gaits with application to a snake-like serial-link structure. *IEEE Trans. Auto. Contr.*, 50(9):1291–1306, 2005.

[9] J. Blair and T. Iwasaki. On the optimal harmonic gait for locomotion of mechanical rectifier systems. *Proc. IFAC World Congress*, 2008.

[10] G. Zhu and R.E. Skelton. Mixed L_2 and L_∞ problems by weight selection in quadratic optimal control. *Int. J. Contr.*, 53(5):1161–1176, 1991.